第9回地震時保有耐力法に基づく橋梁等構造の
耐震設計に関するシンポジウム講演論文集（2006年2月）

SEMI-ACTIVE CONTROL OF SEISMIC-EXCITED NONLINEAR ISOLATED BRIDGES

Tzu-Ying Lee[1] and Kazuhiko Kawashima[2]

[1]Member of JSCE, Post-Doctoral Researcher, Department of Civil Engineering, Tokyo Institute of Technology
(2-12-1 O-Okayama, Meguro, Tokyo 152-8552, Japan)
[2]Member of JSCE, Professor, Department of Civil Engineering, Tokyo Institute of Technology
(2-12-1 O-Okayama, Meguro, Tokyo 152-8552, Japan)

1. INTRODUCTION

Structural control technology has been studied to be effective in reducing seismic responses of isolated bridges[1)-4)]. When isolated bridges are subjected to ground motions with large intensity or unexpected characteristics, not only the isolators but also the columns undergo high hysteretic behavior such that the resulting displacements of the decks become excessively large, which may result in the higher-than-expected seismic force due to the pounding of decks and the $P-\delta$ effect[5)]. In the previous studies[1)-4)], semi-active control systems were studied to effectively reduce seismic responses of isolated bridges. However, the isolators were regarded as either nonlinear elements or hysteretic elements in only several studies with all the columns being assumed to behave linearly. In reality, the columns may exhibit hysteretic behavior under extreme excitations. Hence the objective of this study is to reduce the deck displacement of isolated bridges with nonlinearity at both the columns and isolators by using semi-active control technology.

One means of achieving a semi-active control is to adopt a variable damper, in which the damping coefficient can be regulated. The linear quadratic regulator (LQR) optimal control algorithm and sliding mode control algorithm are selected to command the variable damper herein. A five-span viaduct with high-damping-rubber isolators is analyzed to evaluate the control effectiveness. The results reveal that the variable damper can trace most of the control forces demanded by the LQR control algorithm as well as the sliding mode control algorithm. The control performance in reducing the deck displacement is outstanding using the sliding mode control algorithm as compared with the LQR optimal control algorithm.

2. NONLINEAR ISOLATED BRIDGES

Assuming the deck of a typical isolated bridge is rigid in the longitudinal direction, a column with the effective deck mass on the top can be taken apart as a unit for seismic analysis, as shown in **Fig. 1**. For study of control effectiveness, the column-isolator-deck system may be idealized as a two degree of freedom lumped-mass system. A control device is set between the deck and the column where the isolators are installed.

The column and isolator are assumed to behave nonlinearly, and the damping of the system is assumed as linear viscous herein. The equations of motion of the isolated bridge system may be expressed as

$$\mathbf{M}\ddot{\mathbf{x}}(t)+\mathbf{C}\dot{\mathbf{x}}(t)+\mathbf{F}[\mathbf{x}(t)] = \boldsymbol{\eta}\ddot{x}_g(t)+\mathbf{H}U(t) \quad (1)$$

in which $\mathbf{x}(t),\dot{\mathbf{x}}(t),\ddot{\mathbf{x}}(t)$ are the displacement, velocity and acceleration vectors; $\ddot{x}_g(t)$ is the absolute ground acceleration; $\mathbf{M}$ and $\mathbf{C}$ are mass and damping matrices, respectively; $\mathbf{F}[\mathbf{x}(t)]$ is the

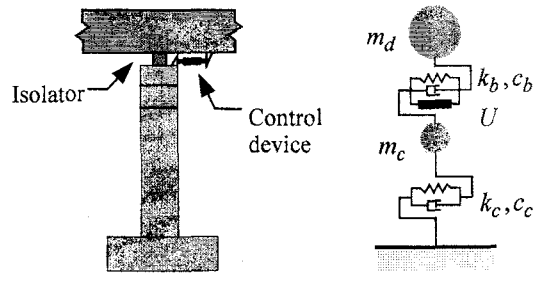

Fig.1 Analytical idealization - 2DOFs system.

nonlinear stiffness vector; $U(t)$ is the control force generated by the control device, and $\boldsymbol{\eta}$ and $\mathbf{H}$ are the location matrices of the excitation and the control force, respectively.

The equations of motion by Eq. (1) can be written based on a state space formulation as

$$\dot{\mathbf{Z}}(t) = \mathbf{g}[\mathbf{Z}(t)] + \mathbf{B}U(t) + \mathbf{W}\ddot{x}_g(t) \tag{2}$$

where $\mathbf{Z}(t) = [\mathbf{x}(t) \quad \dot{\mathbf{x}}(t)]^T$ is the space-state vector; $\mathbf{g}[\mathbf{Z}(t)]$ is a nonlinear function of $\mathbf{Z}(t)$. $\mathbf{g}$, $\mathbf{B}$ and $\mathbf{W}$ are defined as follows:

$$\mathbf{g}[\mathbf{Z}(t)] = \begin{bmatrix} \dot{\mathbf{x}} \\ -\mathbf{M}^{-1}[\mathbf{C}\dot{\mathbf{x}}(t) + \mathbf{F}[\mathbf{x}(t)]] \end{bmatrix};$$

$$\mathbf{B} = \begin{bmatrix} 0 \\ \mathbf{M}^{-1}\mathbf{H} \end{bmatrix}; \quad \mathbf{W} = \begin{bmatrix} 0 \\ \mathbf{M}^{-1}\boldsymbol{\eta} \end{bmatrix} \tag{3}$$

3. CONTROL STRATEGIES

(1) LQR Optimal Control

In this algorithm, the control force $U(t)$ in Eq. (1) is selected by minimizing the quadratic function, over the duration of the excitation, as

$$J = \int_0^{t_f} [\mathbf{Z}^T(t)\mathbf{Q}\mathbf{Z}(t) + RU^2(t)]dt \tag{4}$$

in which $\mathbf{Q}$ is a (4×4) symmetric positive semidefinite weighting matrix and R is a positive weighting scalar.

The optimal solution that minimizes the performance index, as shown in Eq. (4), is obtained under the constraint of the state equations of motion by Eq. (2) as follows

$$U(t) = -0.5R^{-1}\mathbf{B}^T\mathbf{P}\mathbf{Z}(t) = -\mathbf{G}\mathbf{Z}(t) \tag{5}$$

in which $\mathbf{P}$ is the solution of Ricatti equation $\boldsymbol{\Lambda}_0^T\mathbf{P} + \mathbf{P}\boldsymbol{\Lambda}_0 - 0.5\mathbf{P}\mathbf{B}R^{-1}\mathbf{B}^T\mathbf{P} = -2\mathbf{Q}$. Note that the constant Ricatti matrix $\bar{\mathbf{P}}$ is obtained by linearizing the structure at $\mathbf{Z} = 0$ as $\boldsymbol{\Lambda}_0 = \partial\mathbf{g}(\mathbf{Z})/\partial\mathbf{Z}|_{\mathbf{Z}=0}$, neglecting the earthquake excitation $\ddot{x}_g(t)$ and assuming the transient part $\dot{\mathbf{P}}$ equal to zero[6].

(2) Sliding Mode Control

In sliding mode control, the response trajectory is driven into the sliding surface where the motion is stable[7]. In this study, sliding surface, $\mathbf{S}$, is defined as a linear combination of state vector $\mathbf{Z}$ such that

$$\mathbf{S} = \bar{\mathbf{P}}\mathbf{Z}(t) \tag{6}$$

For nonlinear structures, the nonlinear stiffness vector $\mathbf{F}[\mathbf{x}(t)]$ in Eq. (1) can be separated into two parts as

$$\mathbf{F}[\mathbf{x}(t)] = \mathbf{K}\mathbf{x}(t) + \bar{\mathbf{F}}[\mathbf{x}(t)] \tag{7}$$

in which $\mathbf{K}$ = pre-yielding stiffness matrix and $\bar{\mathbf{F}}[\mathbf{x}(t)]$ = nonlinear restoring force vector. The space-state motion equations by Eq. (2) can be written as

$$\dot{\mathbf{Z}}(t) = \mathbf{A}\mathbf{Z}(t) - \mathbf{f}[\mathbf{Z}(t)] + \mathbf{B}U(t) + \mathbf{W}\ddot{x}_g(t) \tag{8}$$

where

$$\mathbf{A} = \begin{bmatrix} \mathbf{0} & \mathbf{I} \\ -\mathbf{M}^{-1}\mathbf{K} & -\mathbf{M}^{-1}\mathbf{C} \end{bmatrix}; \mathbf{f}[\mathbf{Z}(t)] = \begin{bmatrix} \mathbf{0} \\ \mathbf{M}^{-1}\bar{\mathbf{F}}[\mathbf{x}(t)] \end{bmatrix} \tag{9}$$

In the design of the sliding surface, the nonlinear force vector $\mathbf{f}[\mathbf{Z}]$ and the external excitation $\mathbf{W}\ddot{x}_g$ are neglected. However, both $\mathbf{f}[\mathbf{Z}]$ and $\mathbf{W}\ddot{x}_g$ are taken into account in the design of the controller. Sliding surfaces can be determined using pole assignment method or LQR method[7].

To design the controller, the following Lyapunov function is considered

$$V = 0.5\mathbf{S}^T\mathbf{S} \tag{10}$$

The sufficient condition for the sliding mode to occur is given by $\dot{V} = \mathbf{S}^T\dot{\mathbf{S}} \le 0$. From Eqs. (6) and (8), a continuous controller is given by

$$U(t) = \alpha G - \delta\lambda \tag{11}$$

where $G = -(\bar{\mathbf{P}}\mathbf{B})^{-1}\bar{\mathbf{P}}(\mathbf{A}\mathbf{Z} - \mathbf{f} + \mathbf{E})$; $\lambda = \mathbf{S}^T\bar{\mathbf{P}}\mathbf{B}$. Both α and δ are specified by designers with $0 \le \alpha \le 1$.

(3) Saturated Control

When the control force is bounded by a maximum value $U_{\max}$, the saturated control force $U^*(t)$ is given as

$$U^*(t) = \begin{cases} U(t) & |U(t)| < U_{\max} \\ U_{\max} sign(U(t)) & |U(t)| \ge U_{\max} \end{cases} \tag{12}$$

in which $U(t)$ is the active control force required by Eq. (5) or Eq. (11).

(4) Semi-Active Control

When a variable damper is used as the semi-active control device, the control force $V(t)$ from the variable damper is given by

$$V(t) = \xi_b(t)\dot{x}_b(t) \tag{13}$$

where $\xi_b(t)$ is the time-variant damping coefficient and $\dot{x}_b(t)$ is the relative velocity of the isolator.

In semi-active control, the variable damper is expected to provide the demanded control force

$U^*(t)$ by Eq. (12). Therefore, equating Eq. (12) and Eq. (13) yields the demanded damping coefficient of variable damper $\xi_b^*(t)$ as[8]

$$\xi_b^*(t) = \frac{U^*(t)}{\dot{x}_b(t)} \tag{14}$$

It is noted that the control force cannot be commanded directly but viscous coefficient has to be regulated in the variable damper. The external energy required for such control is generally much smaller than that required for the active control.

When the damping coefficient of a variable damper is bounded by a minimum value $\xi_{\min}$ and a maximum value $\xi_{\max}$, the viscous damping coefficient $\xi_b(t)$ has the following constrains

$$\xi_b(t) = \begin{cases} \xi_{\min} & \xi_b^* \le \xi_{\min} \\ \xi_b^* & \xi_{\min} < \xi_b^* < \xi_{\max} \\ \xi_{\max} & \xi_{\max} \le \xi_b^* \end{cases} \tag{15}$$

Therefore, the variable damper not only changes the damping coefficient depending on feedback structural responses to resemble an active system but also functions as a passive energy dissipater.

4. TARGET VIADUCT

An isolated viaduct as shown in **Fig. 2**, which is designed based on Japan Design Specifications of Highway Bridges[9], is analyzed here to investigate the performance of structural control. The superstructure consists of a five-span continuous deck with a total length of 5@40 m = 200 m and a width of 12 m. It is supported by four 12 m tall reinforced concrete columns and two 9.5 m tall abutments. Five high-damping-rubber isolators support the deck per column and abutment.

For study of the control effectiveness, it is idealized as a two degree of freedom lumped-mass system. The effective mass of deck and column are 600 ton and 243.15 ton, respectively. The column and the isolators are assumed to be perfect elastoplastic and bilinear elastoplastic, respectively. The initial stiffness of the column and the five isolators is 112.7 MN/m and 47.6 MN/m, respectively while the yielding displacement is 0.031 m and 0.016 m, respectively. The ratio of post-yielding stiffness to initial stiffness of the isolator is 0.19. The first and second natural periods of the isolated bridge with the initial elastic stiffness are 0.86 sec and 0.24 sec, respectively. The damping ratios of the system are assumed 2% for both modes.

In simulation, the isolated bridge is subjected to two near-field ground motions recorded at JMA Kobe Observatory in the 1995 Kobe, Japan earthquake and Sun-Moon Lake in the 1999 Chi-Chi, Taiwan earthquake as shown in **Fig. 3**. The Bouc-Wen hysteretic model[10] is used to simulate the restoring force of both the column and the isolator.

As shown in **Tables 1 and 2**, the peak deck displacement reaches 0.24 m under JMA Kobe ground motion and 0.55 m under Sun-Moon Lake ground motion as uncontrolled. It is important to note that the isolator exhibits high hysteretic behavior and that the column has a high ductility of eight and a residual displacement of 0.11 m under Sun-Moon Lake ground motion, which results in the

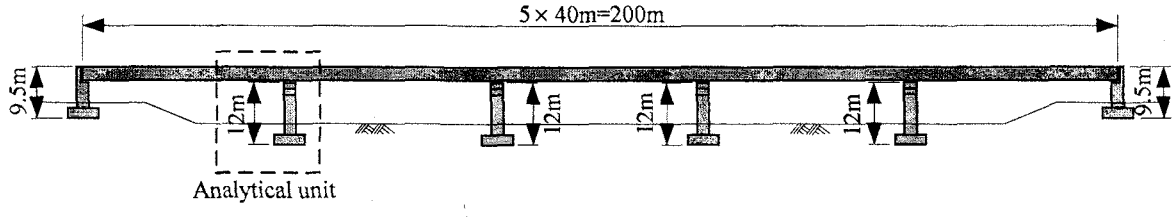

Fig.2 A continuous elevated highway bridge.

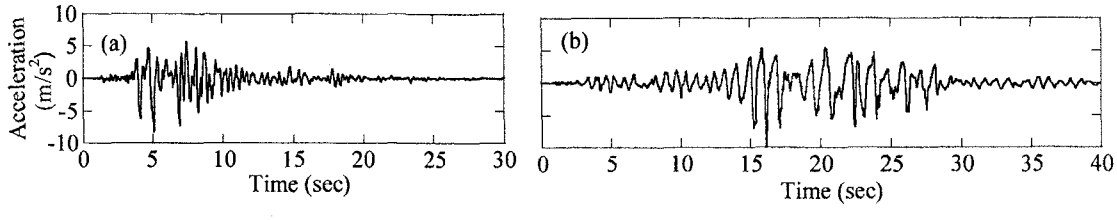

Fig.3 Ground motion records: (a) JMA Kobe observatory, and (b) Sun-Moon Lake.

same magnitude of residual displacement in the deck.

5. SIMULATION RESULTS

With an actuator exerting the active control force by LQR optimum control algorithm, weighting matrix **Q** is *diag*[1,1000,1,1] with off-diagonal elements to be zero and R is 3×10^{-12} in Eq. (4). When using sliding mode control algorithm, the pole assignment method is used to determine the sliding surface where the poles are −30 and $-10\pm25i$. With the sliding mode controller given by Eq. (11), δ is set to be one and α is varied to lead the same peak control force as the LQR controller. The peak responses for both the active controllers are presented in **Tables 1 and 2**. It is observed that both controllers are effective in reducing the peak deck displacement under both ground motions. Especially, the sliding mode control achieves better control performance in reducing the peak deck displacement and column ductility than the LQR optimal control.

Through an extensive parametric study, it is found that larger control force does not further decrease even inversely increases the deck displacement and results in larger column ductility and residual displacement. To avoid such ineffective control, saturated control is thus used based on Eq. (11). The peak deck displacement responses under LQR control and sliding mode control with saturation of the control force, U_{max} = 20% deck weight (1.176 MN), are presented in **Tables 1 and 2**. It is showed that the peak deck displacement is generally the same as that under active control but that the column residual displacement decreases even though the peak control force significantly decreases.

A variable damper based on the LQR control algorithm or the sliding mode control algorithm is used to apply semi-active control force to the isolated bridge. The upper and lower bound of the viscous coefficient of the variable damper, ξ_{max} and ξ_{min} in Eq. (15), is 1.5 MN/m/s and 0.375 MN/m/s, respectively. Weighting parameters in Eq. (4) for the LQR control and the sliding surface and controller parameters in Eqs. (6) and (11) for the sliding mode control are assumed as same as those of the previous active control. The saturation of control force, U_{max}, is 20% of the deck weight.

Figure 4 compares the control force and the deck displacement response of the isolated bridge among uncontrolled system, active controlled and semi-

Table 1 Peak control force and peak responses under JMA Kobe record.

Control method	Control force (kN)	Deck displacement (m)	Isolator ductility	Column ductility	Column residual displacement (m)
Uncontrol	-	0.24	14	1.6	0.02
Active LQR control	1910	0.17	8	2.0	0.03
Active sliding mode control	1910	0.12	8	1.4	0.01
Active LQR control with saturation	1176	0.18	10	1.6	0.02
Active sliding mode control with saturation	1176	0.12	8	1.3	0.01
Semi-active LQR control with saturation	1176	0.17	9	1.4	0.01
Semi-active sliding mode control with saturation	1176	0.14	9	1.1	0.00
Passive control with maximum damping	1658	0.15	8	1.5	0.02

Table 2 Peak control force and peak responses under Sun-Moon Lake record.

Control method	Control force (kN)	Deck displacement (m)	Isolator ductility	Column ductility	Column residual displacement (m)
Uncontrol	-	0.55	25	8.0	0.11
Active LQR control	1951	0.37	11	8.0	0.21
Active sliding mode control	1951	0.31	14	4.5	0.10
Active LQR control with saturation	1176	0.34	15	4.0	0.07
Active sliding mode control with saturation	1176	0.32	16	4.0	0.09
Semi-active LQR control with saturation	1176	0.34	16	3.4	0.07
Semi-active sliding mode control with saturation	1176	0.33	16	3.1	0.06
Passive control with maximum damping	2045	0.37	14	4.9	0.12

active controlled systems using sliding mode control algorithm under Sun-Moon Lake ground motion. The damping coefficient of the variable damper is also presented here. As observed from **Fig. 4**, the control force by the actuator and the variable damper is virtually the same except at few instants. The force difference between two devices can be attributed to two reasons. One is that the variable damper is intrinsically an energy dissipation device and cannot add energy to the structural system while the actuator can generate arbitrary force no matter how the control force provides energy. The other reason is that the damping coefficient of the variable viscous damper is bounded by Eq. (15). In spite of slight discrepancy, the semi-active control achieves similar performance to the active control. Under semi-active control, the peak deck displacement of the bridge reduces to 0.33 m and the residual displacement reduces to 0.06 m, which are almost identical to those under active control.

The peak responses of the semi-active control are presented in **Tables 1 and 2** as well. It is seen that the semi-active control achieves comparable performance in reducing the peak deck displacement, peak column displacement and column residual displacement to the active control. In addition, **Tables 1 and 2** also show the peak responses while the variable damper is set to maintain the maximum damping coefficient ξ_{max} at all times, called passive control with maximum damping (PCMD). The results reveal that the semi-active control based on the sliding mode control algorithm is more effective than PCMD under both ground motions. The semi-active control based on the LQR control algorithm presents better performance than PCMD under Sun-Moon Lake ground motion but less performance than PCMD under JMA Kobe ground motion. However, it is noted that the semi-active control generally achieves the best control performance on the column residual displacement.

6. CONCLUSIONS

The effectiveness of seismic displacement response control was studied for a nonlinear isolated bridge exhibiting inelastic response at both the column and isolator under near-field ground motions. The semi-active control using a variable damper based on either the LQR optimal control algorithm or the sliding mode control algorithm, was investigated and compared with the active control. Analyzed was a five-span viaduct with high-damping-rubber isolators. The following

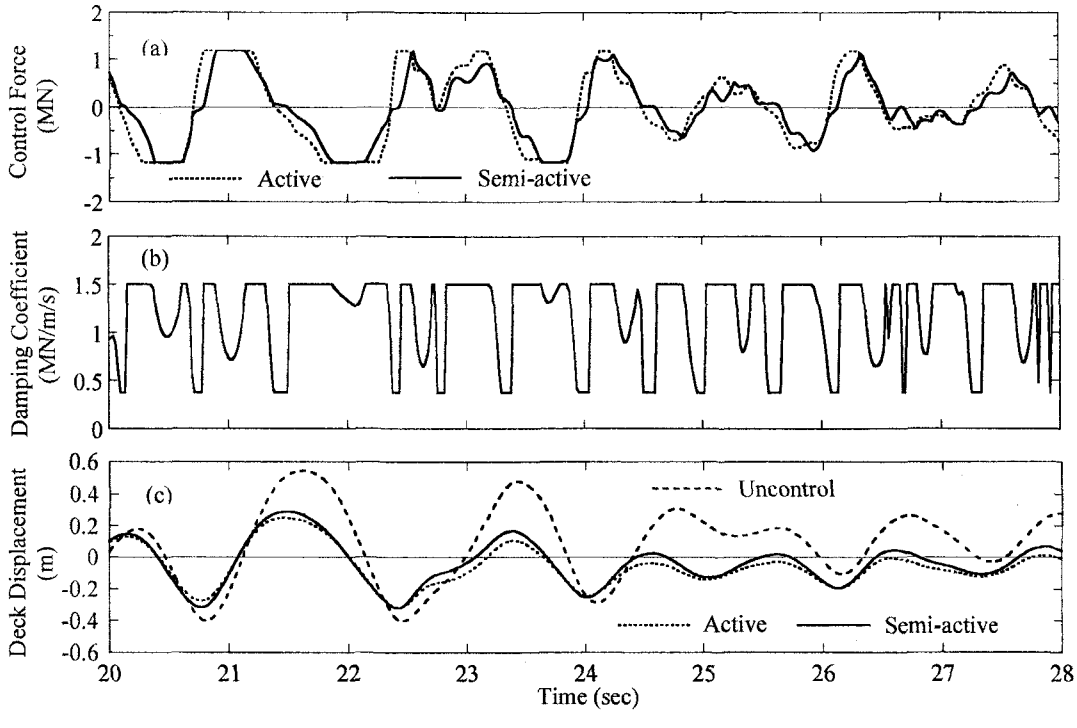

Fig.4 Comparison of the control force and deck displacement between active control and semi-active control based on the sliding mode control: (a) control force, (b) damping coefficient of variable damper, and (c) deck displacement.

conclusions may be derived from the results presented herein.

(1) The semi-active control with a variable damper based on either the LQR control algorithm or the sliding mode control algorithm is effective in reducing the peak deck displacement and provides comparable control performance to the active control using an actuator.

(2) The semi-active control based on the sliding mode control algorithm presents more effective performance than that based on the LQR control algorithm.

(3) The semi-active control generally shows better performance than the passive control with setting the variable damper to remain at the maximum damping coefficient. The column residual displacement is smaller under the semi-active control than under the passive control with maximum damping.

7. ACKNOWLEDGEMENTS: The authors acknowledge the support to the first author during the doctoral study from the Center for Urban Earthquake Engineering in Tokyo Institute of Technology, Tokyo, Japan.

REFERENCES

1) Kawashima, K. and Unjoh, S.: Seismic Response Control of Bridges by Variable dampers, *J. Struct. Eng.*, ASCE, Vol.120, pp. 2583-2601, 1994.

2) Yang, J.N., Wu, J.C., Kawashima, K. and Unjoh, S.: Hybrid Control of Seismic-excited Bridge Structures, *Earthq. Eng. Struct. D.*, Vol.24, pp. 1437-1451, 1995.

3) Erkus, B., Abe, M. and Fujino, Y.: Investigation of semi-active control for seismic Protection of Elevated Highway Bridges, *Eng. Struct.*, Vol.24, pp. 281-293, 2002.

4) Sahasrabudhe, S.S. and Nagarajaiah, S.: Semi-active Control of Sliding Isolated Bridges Using MR Damper: an Experimental and Numerical Study, *Earthq. Eng. Struct. D.*, Vol 34, pp. 965-983, 2005.

5) Priestley, M.J.N., Seible, F. and Calvi, G.M.: *Seismic Design and Retrofit of Bridges*, John Wiley & Sons, USA, 1996.

6) Yang, J.N., Li, Z. and Vongchavalitkul, S.: Generalization of Optimal Control Theory: Linear and Nonlinear Control, *J. Eng. Mech.*, ASCE, Vol.120, pp. 266-283, 1994.

7) Yang, J.N., Wu, J.C. and Agrawal, A.K.: Sliding Mode Control for Nonlinear and Hysteretic Structures, *J. Eng. Mech.*, ASCE, Vol.121, pp. 1330-1339, 1995.

8) Symans, M.D. and Constantinou, M.C.: Seismic Testing of a Building Structure with a Semi-Active Fluid Damper Control System, *Earthq. Eng. Struct. D.*, Vol.26, pp. 759-777, 1997.

9) Japan Road Association: *Design specifications of highway bridges, part V seismic design*, Tokyo: Maruzen, 1996.

10) Wen, Y.K.: Method for Random Vibration of Hysteretic System, *J. Eng. Mech. Division*, ASCE, Vol.102, pp. 249-263, 1976.